Research Square

Preprints are preliminary reports that have not undergone peer review.
They should not be considered conclusive, used to inform clinical practice,
or referenced by the media as validated information.

Optimizing produced water reinjection pump energy consumption using variable frequency regulation

Olasunkanmi Oluwadara Olawole
Durban University of Technology
Oluwatoyin Joseph Gbadeyan
toyin2good@gmail.com

Collin College
Charles Deigh
Oando Energy Resource Nigeria Limited
Oludolapo Akanni Olanrewaju
Durban University of Technology

Research Article

Keywords: Produced Water Re-injection, Variable Frequency Drive, Hydraulic Mismatch, Energy Optimization, Transient Simulation

Posted Date: July 9th, 2026

DOI: https://doi.org/10.21203/rs.3.rs-10195177/v1

License: This work is licensed under a Creative Commons Attribution 4.0 International License.
Read Full License

Additional Declarations: No competing interests reported.

Optimizing produced water reinjection pump energy consumption using variable frequency regulation

***Olasunkanmi Oluwadara Olawole*[1], *[*]*Oluwatoyin Joseph Gbadeyan*[2,3], *Charles Deigh*[4], Oludolapo Akanni Olanrewaju[1,2]**

[1]Department of Industrial Engineering, Durban University of Technology 4000, South Africa.

[2]Institute of Systems Science, Durban University of Technology, Durban 4000, South Africa

[3]Engineering Technology, Collin College, Plano Texas, United State

[4]Oando Energy Resource Nigeria Limited, Lagos, Nigeria

*Corresponding Author: (***Oluwatoyin Joseph Gbadeyan)** toyin2good@gmail.com

Abstract

In mature oil fields, the hydraulic load on Produced Water Re-injection (PWRI) pumps is highly dynamic, driven by fluctuating reservoir backpressure and varying wastewater production rates. However, standard mechanical design practices typically size centrifugal injection pumps for the "worst-case" peak pressure condition expected at the end of the field's life. This static design philosophy creates a severe hydraulic mismatch during the early-to-mid operational years, forcing operators to dissipate excess hydraulic energy across choke valves. This practice not only results in substantial thermodynamic losses but also subjects the mechanical system to excessive throttling, vibration, and wear. This study analyzes the mechanical and energetic advantages of replacing conventional Fixed-Speed Drive (FSD) throttling control with a Staged Variable Frequency Drive (VFD) strategy. A coupled hydraulic-mechanical simulation was developed to model the transient interaction between the surface pumping system and the subsurface reservoir load over a 20-year lifecycle. The model integrates a dynamic system head curve derived from field data with pump performance curves governed by Affinity Laws. Results indicate that the reservoir backpressure fluctuates significantly (3,500–4,200 psi), causing fixed-speed pumps to operate far from their Best Efficiency Point (BEP). The proposed variable speed control strategy eliminates throttling losses, reducing the lifecycle electricity requirement from 177.45 GWh to 151.22 GWh—a 14.8% relative reduction in total system energy consumption. Furthermore, based on established turbomachinery reliability physics, theoretical projections suggest this optimization mitigates mechanical stress on valve trims and piping infrastructure. While the primary benefit is thermodynamic optimization, the associated reduction in power consumption yields an estimated operational cost saving of $3.15 million, validating the strategy as both mechanically superior and economically viable.

Keywords: Produced Water Re-injection, Variable Frequency Drive, Hydraulic Mismatch, Energy Optimization, Transient Simulation.

1: Introduction

1.1 Mechanical Challenges in High-Pressure Injection

Produced Water Re-injection (PWRI) systems represent one of the most demanding mechanical loads in the upstream oil and gas industry. High-energy multistage centrifugal pumps serve as the primary drivers in these facilities, engineered to generate hydraulic heads often exceeding 3,000 meters to overcome deep subsurface hydrostatic and formation pressures [1]. In standard turbomachinery design, these pumps are engineered to operate with optimal hydraulic stability at a specific Best Efficiency Point (BEP). At this point, the incidence of the fluid corresponds perfectly to the geometry of the impeller vanes, resulting in minimum flow separation and neutralized radial loads [2].

However, the operational reality of mature fields compels these pumps to operate under highly variable hydraulic loads that deviate significantly from their design conditions. Standard industry practice dictates that injection pumps are rated for the 'worst-case' hydraulic duty specifically, the highest anticipated reservoir parting pressure and maximum water disposal rates at the field's end-of-life [3]. This static design philosophy introduces a fundamental mechanical mismatch during the early-to-mid years of operation, a period characterized by significantly lower system head requirements.

To control this surplus energy, facilities normally use discharge throttling method by partially closing a control valve part way to deliberately raise the system resistance curve. Thermodynamically, throttling is an isenthalpic process, which irreversibly transforms useful hydraulic work into entropy (heat) and noise, rather than pressure recovery [4]. This is an inefficient control method that poses very critical mechanical integrity hazards. As research indicates, operating centrifugal pumps at a significant distance to the left of the BEP (throttled condition) causes internal flow recirculation at the eye and discharge tip of the impeller. This hydraulic instability induces high-frequency pressure pulsations and undue radial shaft deflection, which in turn accelerates the fatigue failure of mechanical seals and bearings [2]. Moreover, the highly turbulent flow across the throttling valve trim results in cavitation and erosion damage, necessitating frequent component replacement [5].

1.2 The Dynamic Load Profile

As opposed to the fixed-point industrial pumping tasks, the “System Head Curve of a water injection network is a dynamic parameter that changes constantly throughout the life of the asset. Two major underlying factors driving this evolution are subsurface repressurization of reservoirs and deterioration of injectivity. Obibuike et al [6] conducted detailed reservoir simulations to show that the reservoir pore pressure (P_{res}) is very dynamic; it can drop to extreme low levels (e.g., 4,500 psi to 3,500 psi) during the initial depletion (before injection support commences) and increase steadily once voidage replacement begins.

For illustration, during the initial development stages of an oil field such as the ABX2 of the Niger Delta, the generated flow of water is low (< 2,000 bbl/d). Simultaneously, the pump buildup of solids and oil droplets at the nearwellbore area generates a filter cake which raises the skin factor and the hydraulic resistance necessary to sustain injection rates. This dynamic load poses a major threat of mechanical oversizing during the initial years of production. As an illustration, during the initial development stages of an oil field such as the ABX2 of the Niger Delta, the generated water flow is low (< 2,000 bbl/d) yet the pump is engineered to reach a late-stage capacity greater than 19,000 bbl /d. When a large-capacity pump is used at such low flow rates (usually less than 30 percent of the BEP) it forces the machine into a zone of hydraulic instability called “the Minimum Continuous Stable Flow” limit. Prolonged operation in this zone causes thermal accumulation in the casing and damaging cavitation which can erode holes in the impeller vanes and obliterate hydraulic efficiency. The associated mechanical degradation due to this load mismatch is frequently diagnosed as a maintenance problem rather than an inherent design problem. Modern predictive simulation frameworks, such as those reviewed by Wan et al. [8], suggest that this design mismatch can be mitigated by modeling the equipment's lifecycle performance against dynamic boundary conditions.

1.3 Study Framework

Consequently, the primary objective of this research is to maximize the hydraulic performance of PWRI surface facilities by substituting conventional fixed throttling controls with a dynamic Staged Variable Frequency Drive (VFD) strategy. To achieve this, we developed a fully coupled hydraulic-mechanical simulation that models the transient interaction between the surface pumping system and the subsurface reservoir load over a 20-year lifecycle.

The scope of this analysis is specifically confined to the optimization of the surface mechanical system comprising centrifugal pumps, electric motors, and flow control logic treating the reservoir pressure and flow rate as dynamic boundary conditions. While the study integrates a detailed techno-economic evaluation to validate financial viability, the primary focus remains on quantifying the reduction in Specific Energy Consumption (SEC, measured in kWh per barrel) and lifecycle electricity demand, while inferring the theoretical alleviation of mechanical stresses (vibration and valve wear) using Best Efficiency Point (BEP) deviation as a proxy indicator.

The primary objective of this research is to maximize hydraulic performance by substituting conventional fixed throttling with a dynamic Staged-VFD strategy. The novelty of this work resides in its coupled approach; while previous efforts often overlook the mechanical implications of subsurface challenges on surface machinery, this study integrates turbomachinery reliability physics with transient reservoir boundary conditions. By focusing on a 20-year lifecycle in the Niger Delta, the framework identifies the specific energy and mechanical costs of the Hydraulic Mismatch, offering a data-driven path to optimizing both energy consumption and equipment longevity.

2 Review of Related Works

Although optimization of water injection systems has been extensively researched, the current literature tends to adopt a decoupling of surface facility and the subsurface reservoir as a domain. The review of the recent studies reveals that there are gaps in technology, which this research seeks to fill.

2.1 The drawbacks of Static Lifecycle Costing

Recent research by Elembaby et al. [3] offered a solid lifecycle cost analysis (LCC) framework in the case of mature waterfloods. Their analysis was able to prove the cost-effectiveness of

facility right-sizing. Nevertheless, their model concentrated on the financial measures, but not the environmental aspect. Recently, Gao et al [9] emphasized that the optimization of modern facilities has to consider the carbon intensity of power generation. This aligns with the 'Water-Energy-Carbon Nexus' framework proposed by Gómez-Gardars et al [10], which argues that energy savings in water injection must be directly correlated to emissions reduction. Moreover, the phenomena of the Rising Water Cut and injectivity decline seen in the Niger Delta cannot be modeled by the non-dynamic models and therefore, consistently underestimates the power demand and carbon footprint.

2.2 Weaknesses in Mechanical Reliability Modeling

Aladeitan et al [7] in the case of the Niger Delta have conducted comprehensive reservoir surveillance in which the relationship between the age of the mature field and exponentially rising water production was identified. Their work was correct in the definition of the subsurface challenge, but the mechanical implications on surface machinery were not considered. This study demonstrates that running pumps under these kinds of variable hydraulic loads without speed regulation causes severe radial to thrust and vibration [11, 12]. The current field research does not pay much attention to this aspect of the physics of reliability, and the pumps are still regarded as steady-state boxes instead of moving tribological systems.

2.3 Geomechanical Oversimplifications

Zhou et al. [2] offered a contribution to the field by developing a network optimization model of surface pipelines. Although their model was successful in reducing the frictional losses, they have used a linear hydraulic model which fails to simulate nonlinear geomechanical effects. Recent high-pressure appraisals by Wang et al [13] show a significant change in system curve of injection wells by thermal fracturing. Failure to account for this variable injection pressure limit may result in pump schedules that unintentionally violate the formation's fracture-gradient constraints (as seen in prior static network models).

2.4 Position of Current Study

The current research fills these gaps in identified research by the creation of a fully coupled hydraulicmechanical model. This study is unlike Elembaby et al [3], which incorporates the sustainability metrics proposed by Gao et al [9]. It substitutes the stagnant mechanical

assumptions of Aladeitan et al [7]. with the dynamic reliability physics of Li et al [11] and it acknowledges geomechanical fracture constraints emphasised by Wang et al [13].

To address the limitations identified in previous research, this study proposes several viable solutions aimed at closing the gap between surface facilities and reservoir dynamics:

- **Coupled Hydraulic-Mechanical Modeling:** Unlike prior decoupled efforts, this research utilizes a transient simulation that links subsurface geomechanical behavior directly to surface mechanical reliability indicators.

- **Staged-VFD Architecture:** To manage the extreme 39:1 turndown ratio that frequently forces single pumps into unstable operating zones, a staged capacity approach is introduced to ensure continuous operation near the Best Efficiency Point (BEP).

- **Mechanistic Energy-Water Nexus Analysis:** The study utilizes Deep Bed Filtration (DBF) kinetics to provide a data-driven solution for quantifying the energy penalty of poor filtration.

- **Application of Reliability Physics:** By integrating the Stepanoff empirical relation, this work provides a framework for translating hydraulic mismatch into physical radial thrust forces, allowing for the prediction of mechanical seal integrity.

3 Simulation Framework and Control Strategy

The paper will use a deterministic simulation model to assess the mechanical performance of a Produced Water Re-injection (PWRI) system when subjected to transient operating conditions. The methodology is designed in such a way that the surface pumping machinery is isolated as the main control volume, and the behaviour of the subsurface reservoir is considered as a dynamic boundary condition. The simulation model combines three interacting mathematical models, including a hydraulic load model of the reservoir and piping network, a mechanical

performance model of the centrifugal pump characteristics, and a control logic algorithm of comparing Fixed-Speed Drive (FSD) operation to Variable Frequency Drive (VFD) operation.

3.1 Hydraulic Load Characterization

Accuracy of any optimization model in mechanical systems engineering is directly related to the fidelity of the load profile. In the case of a PWRI system, the load is not a constant value but a time-varying hydraulic demand that is imposed by the subsurface environment. The paper incorporates the hydraulic load (H_{req}) as a dynamic boundary condition and it varies with a 20-year dynamic operational life based on three main variables, which includes the pore pressure of the reservoir, the desired disposal flow and the rheological characteristics of the fluid.

3.1.1 Reservoir Backpressure Profile

The major resistance to the injection pump is the pressure of the pore in the reservoir (P_{res}). This contrasts with surface storage tanks where the fluid in the tanks has a stable static head, whereas the pressure of the fluid in a reservoir varies dramatically as a result of interactions between fluid withdrawal (production) and fluid replacement (injection). To obtain a representative load profile to use in fixed simulation, the field development study of Field ABX2 in the Niger Delta was used to extract the data of the pressure as was modeled by [6]. The pressure profile has three different mechanical phases:

1. **Depletion Phase (Years 0–3):** Early production leads to the instantaneous drop of pressure to a bottom of about 3,500 psi of the original production reservoir pressure (P_i ≈ 4,500 psi). This, mechanically, is also a time span during which the necessary pump discharge head is reduced, and a possible condition of run-out (high flow, low head) would occur otherwise.

2. **Repressurization Phase (Years 4–8):** When water injection is started to fill in the voidage, the pressure of the reservoir rises sharply, as the pressure rises to 3,600 psi up to 4,100 psi. A substantial rate of change (dP/dt) on the pumping system is applied at this stage.

3. **Stabilization Phase (Years 9–20):** The pressure level off at near 4,200 psi due to the reservoir entering a state of dynamic equilibrium.

This behavior of the transient pressure ($P_{res}(t)$) is the main forcing term of the mechanical simulation which determines the lowest possible discharge pressure that the surface pumps need to overcome to guarantee injectivity.

3.1.2 Wastewater Disposal Rate

The size of the pumps is determined by the volumetric flow rate (Q) necessary to pump the wastewater produced by the production separators. With a disposal-based environment, the injection system should be able to take the entire waste stream to eliminate bottlenecks in production. According to the data provided by Aladeitan et al. [7] and Obibuike et al. [6], there exists a so-called "Rising Water Cut" that is characteristic of old sandstone reservoirs.

The simulation assumes a disposal rate that increases at a slow rate in the first year of 500 bbl/d to the highest rate of 19,500 bbl/d which is reached in Year 20. This 39 times increment in volumetric flow presents a huge Turndown Ratio demand on the mechanical equipment. A fixed speed pump that was rated at the final flow rate (19,500 bbl/d) would act at less than 5 percent of its Best Efficiency Point (BEP) capacity in the initial one year. The extreme partial-load operation has been known to cause serious recirculation and cavitation damage and therefore, the need to adopt a flexible mode of control.

3.1.3 Fluid Rheology

Proper hydraulic power computation needs to have a perfect definition of the physical properties of the fluid. Salt and temperature cause the produced water to be treated as a Newtonian fluid that is different to fresh water. Based on samples from Niger Delta flow stations characterized by [14], the following properties were used in the simulation:

- **Density (ρ):** 1007 kg/m^3 (Representing moderate salt content and dissolved solids).
- **Viscosity (μ):** 0.7 cP (Dynamic viscosity at a standard injection temperature of 36°C).

These rheological constants are essential in the computation of Reynolds number and other following factors of friction in the transmission pipeline.

The complete set of simulation parameters is summarized in **Table 1**

Table 1: Summary of Hydraulic and Mechanical Simulation Parameters

Parameter	Value	Unit	Source/Derivation
Fluid Properties			
Produced Water Density (ρ)	1007	kg/m^3	[14]
Dynamic Viscosity (μ)	0.70	cP	@ 36°C
Piping System			
Flowline Length (L)	5,000	m	Equivalent Length
Pipe Internal Diameter (D)	0.15	m	Schedule 40 Steel (6-inch)
Roughness Coefficient (C)	120	-	Hazen-Williams
Static Lift (ΔZ)	50	m	Pump to Wellhead
Pump Specifications			
Pump Efficiency (η_{pump})	75	%	BEP Estimate
Motor Efficiency (η_{motor})	95	%	NEMA Premium [15]
VFD Efficiency (η_{VFD})	97	%	Standard Drive Loss
Economic Factors			
Electricity Tariff	0.12	$/kWh	Industrial Rate [16]
Project Lifecycle	20	Years	Simulation Horizon

3.2 Governing Mathematical Formulations

Simulation of the interaction between the prime mover and the hydraulic load was done rigorously based on the principles of conservation of energy and mass. The surface injection plant is a control volume which is framed by the pump suction header and the wellhead injection flange. To ensure strict dimensional homogeneity across the diverse hydraulic and mechanical relationships, all field-standard inputs (e.g., psi, bbl/d) are mathematically converted into consistent System International (SI) base units (e.g., Pascals, m³/s, kg) prior to internal computation within the simulation algorithms. Final outputs are subsequently translated back into standard oilfield nomenclature for industry interpretation.

3.2.1 Conservation of Energy (Bernoulli's Principle)

The amount of energy needed is calculated by using the Generalized Bernoulli Equation between the pump suction (Point 1) and the discharge of the wellhead (Point 2). Assume incompressible adiabatic flow of water brine that is produced:

$$\frac{P_1}{\rho g} + \frac{v_1^2}{2g} + z_1 + H_{pump} = \frac{P_2}{\rho g} + \frac{v_2^2}{2g} + z_2 + h_f + \Sigma h_m \tag{1}$$

Where:

- $P/\rho g$ indicates the pressure head.
- $v^2/2g$ is the head of velocity (kinetic energy).
- z represents geodetic elevation.
- h_f and Σh_m are large friction losses and small fitting losses respectively.

Because the pipe diameter both at the suction and discharge is given a constant ($D_1 \approx D_2$)), the change in velocity head is insignificant ($\Delta v \approx 0$). Rearrangement to find the necessary Pump Head H_{sys}):

$$H_{sys} = (z_2 - z_1) + \frac{P_{res}(t) + \Delta P_{skin}}{\rho g} + h_f(Q) \tag{2}$$

This derivation proves that the load is the sum of the statical lift (ΔZ), the dynamic condition of the reservoir (P_{res}) and the friction that is dependent on the flow. In fixed speed systems, according to De Oliveira et al [4], the imbalance between $H_{pump} > H_{sys}$ leads to energy losses in the form of heat through the choke valve.

3.2.2 Flow Regime and Friction Characterization

To check the applicability of the Hazen-Williams friction model, the flow regimen was identified in terms of the Reynolds Number (Re). . For the produced water with density ρ = 1007 kg/m^3 and viscosity μ = 0.7 cP flowing through a 0.15 m pipe at peak rates (Q = 19,500 bbl/d or 0.035 m^3/s):

$$Re = \frac{\rho v D}{\mu} = \frac{4\rho Q}{\pi \mu D} \tag{3}$$

Substituting the fluid properties yields $Re \approx 1.2\times10^5$. Since $Re \gg 4{,}000$, the flow is fully turbulent. The frictional head loss (h_f) is therefore no longer dependent on viscosity but mostly on the roughness of the pipes. The Hazen-Williams equation is hence used as the governing resistance equation:

$$h_f = \frac{10.67 \cdot L \cdot Q^{1.852}}{C^{1.852} \cdot D^{4.87}} \tag{4}$$

3.2.3 VFD Scaling Laws (Affinity Derivation)

The Pump Affinity Laws that are based on dimensional analysis of turbomachinery are the controlling factors in the energy saving in Scenario B. In the case of a centrifugally controlled flow, capacity (Q), Head (H) and Power (P) are proportional to the ratio of rotational speeds 2 / from the rotational speed ratio $\alpha = N_2/N_1$:

$$\frac{Q_2}{Q_1} = \alpha, \quad \frac{H_2}{H_1} = \alpha^2, \quad \frac{P_2}{P_1} = \alpha^3 \tag{5}$$

The proposed optimization is a cubic ($P \propto N^3$) relationship that is the most important mathematical driver. The theoretical power reduction is almost 50 percent ($0.8^3 = 0.512$) with the speed decreasing by only 20 percent ($\alpha = 0.8$). This non-linear scaling is what causes the extent of the savings as observed in the simulation results.

3.3 Mechanical System Modeling

Trying to emulate the interplay between the prime mover and the hydraulic load, the surface injection facility was described as a non-linear network of three major mechanical subsystems, namely, the transmission pipeline, the flow control mechanism, and the centrifugal pump unit. These subsystems were governed by the principles of fluid mechanics and conservation of energy derived to obtain the governing equations.

3.3.1 The System Head Equation

The Total Dynamic Head (H_{sys}) is the sum of all mechanical energy (divided by weight) that the pump is supposed to add to the fluid so that it passes all resistances down the pipe. The PWRI system head is variable in time as opposed to the static industrial pumping system because it depends on the transient reservoir pressure $P_{res}(t)$. The governing equation of the head required in system at time step t is given as:

$$H_{sys}(Q,t) = \Delta Z + \frac{P_{res}(t) + \Delta P_{skin}(t)}{\rho g} + h_f(Q) \quad (6)$$

Where:

- ΔZ: The vertical height difference between pump centerline and wellhead datum (50 m).
- $P_{res}(t)$: The instantaneous reservoir pore pressure, converted from field psi to Pascals (Pa) for computational consistency.
- $\Delta P_{skin}(t)$: The extra pressure drops necessary to surmount near-wellbore formation damage, evaluated in Pascals (Pa).
- $h_f(Q)$: The dynamic frictional head loss in surface piping network (m).

This equation points out that mechanical load is a combination of a non-fluxing (elevation) component, a dynamic boundary condition (reservoir pressure) and flow-dependent resistance (friction and skin).

3.3.2 Friction Loss Model (Hazen-Williams)

The Hazen-Williams empirical formula was used to measure the amount of energy that dissipated because of fluid turbulence inside the transmission lines which are of high pressure. In optimization of water injection networks, e.g., by Zhou et al. [2], this model is extensively mentioned because it is a strong representation of turbulent flow in steel pipes. Frictional loss of head (h_f) is non-linearly dependent on the flow rate (Q):

$$h_f = \frac{10.67 \cdot L \cdot Q^{1.852}}{C^{1.852} \cdot D^{4.87}} \quad (7)$$

Where:

- L: Equivalent length of injection flowline (5,000 m) including the linear length of the pipe and equivalent length of fittings and bends.
- D: Pipe internal diameter (0.15 m) which is a standard 6-inch schedule 40 carbon steel pipe.
- C: Hazen-William's roughness coefficient (120), a property of lined steel pipe in service in corrosive service interchange of produced water.

The power law ($h_f \propto Q^{1.852}$) shows that the friction losses are insignificant at the low flow initial life of the field but a major energy consuming element at the peak disposal time.

3.3.3 Pump Performance Model

The injection system's prime mover consists of a multistage centrifugal pump. To enable continuous transient simulation, the hydraulic performance of the pump cannot be treated as a static point; it must be modeled as a continuous characteristic curve. To achieve this, empirical performance data from a commercial API 610 injection pump (rated for 20,000 bbl/d) was digitized. A Least Squares polynomial regression algorithm was then applied to the digitized manufacturer curves to extract the specific coefficients for the Head-Flow ($H-Q$) and Power-Flow ($P-Q$) relationships. At the specified rated rotational speed (N_{rated} = 2,950 rpm) the hydraulic head generated by the impeller is modeled by the resulting second-order polynomial:

$$H_{pump}(Q) = a_0 + a_1 Q + a_2 Q_2 \tag{8}$$

a_0 has a meaning of shut-off head (maximum pressure at zero flow) and a_2 has a meaning of curvature of the hydraulic profile of the impeller. In a similar fashion the Brake Horsepower (BHP) needed by the pump shaft is modeled as follows:

$$P_{pump}(Q) = b_0 + b_1 Q + b_2 Q_2 \tag{9}$$

Mechanical Degradation Factors: Centrifugal pumps are normally designed to achieve optimal operation at a set Best Efficiency Point (BEP). Working the pump well to the left of the BEP as is typical during the first years of a field as the flow is modest is severe mechanical stress. Survey results by Rossini et al [5] and others suggest that throttled operation results in internal flow recirculation, which is manifested in high frequency vibration and cavitation erosion of the impeller vanes. The simulation model takes this into consideration by monitoring the “Operating Point” deviation of the BEP and using it as a proxy of mechanical integrity risk.

The characteristic curves for the staged pumps are shown in **Figure 1**

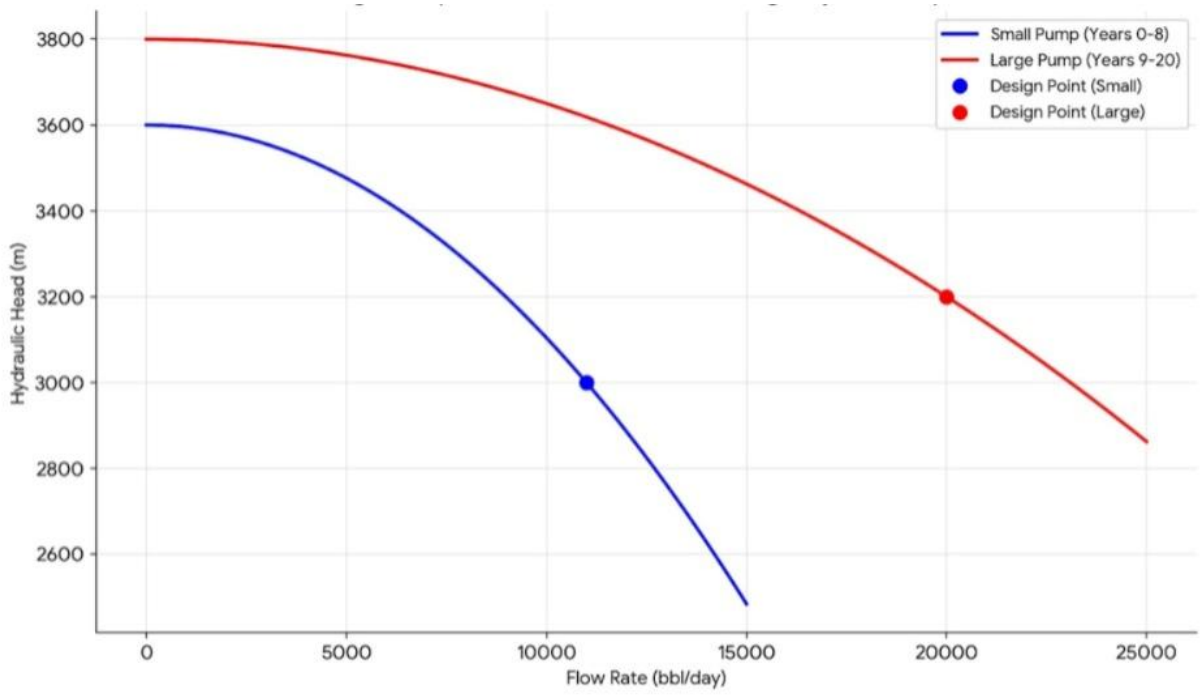


Figure 1: Hydraulic Performance Curves of Staged Injection Pumps. The blue curve represents the Small Pump optimized for early-life low flow rates, while the red curve represents the Large Pump designed for peak late-life demand. Dots indicate the Best Efficiency Point (BEP) for each unit.

3.3.4 Reliability Physics: Radial Thrust Modeling

The major mechanical implication of centrifugal pumps that run off design is the creation of hydraulic radial thrust. At the Best Efficiency Point (BEP), the pressure distribution of the impeller volume is balanced, and the net radial force is zero. At other flow rates (Q) other than the design flow (Q_{BEP}), the pressure profile is asymmetric to form a net Radial Force (F_r) which is orthogonal to the axis of the shaft flow.

The Stepanoff empirical relation, which had been demonstrated to work with multistage pumps was applied to the radial thrust to measure the mechanical stress on the bearings and seals during the throttled (low flow) years, as shown by Li et al [11]:

$$F_r = K_r \cdot H \cdot D_2 \cdot b_2 \cdot \frac{\rho g}{1000} \tag{10}$$

Where:

- F_r: Radial Thrust Force (kN).
- H: Pump Head at the operating point (m).
- D_2: Impeller outer diameter (0.45 m).
- b_2: Impeller outlet width (0.004 m).
- K_r: Radial Force Coefficient, defined as:

$$K_r = 0.36 \cdot \left[1 - \left(\frac{Q}{Q_{BEP}}\right)^2\right] \tag{11}$$

Mechanical Impact Analysis:

Under the Fixed-Speed case in the first year (Year 1), the pump will be running at about 5 percent of its potential ($Q/Q_{BEP} \approx 0.05$)). At this state, the coefficient K_r is at its highest (0.36), and the pump head H is at its shut-off peak (≈ 3,800 m). To compute the force in this scenario:

$$F_{r,max} \approx 0.36 \cdot 3800 \cdot 0.45 \cdot 0.004 \cdot \frac{1007 \cdot 9.81}{1000} \approx 24.3\,\text{kN} \tag{12}$$

The shaft deflection is extremely high with the presence of a constant radial load of 24.3 kN (2.48 tonnes) on the pump shaft. However, as mentioned by Simon et al [12] such deflection is beyond the clearance limits of conventional API 682 mechanical seals and results in contact of the face, thermal cracking and early leakage. This calculation demonstrates the severe hydraulic imbalance inherent in low-flow, fixed-speed operations. While direct physical fatigue analysis is outside the scope of this simulation, applying the Stepanoff empirical relation strongly indicates that the resulting radial loads theoretically exceed the clearance limits of conventional API 682 mechanical seals. Thus, early-life seal failures in such systems are inferred as a predictable outcome of hydraulic mismatch rather than isolated mechanical defects [17, 18]. The theoretical contrast in radial thrust generation between the fixed and staged scenarios over the lifecycle is visually summarized in Figure 2.

3.4 Control Strategy Algorithms

To measure the mechanical and energetic difference between the design philosophy formed using a static design and the dynamic adaptive control, this paper models two different scenarios of operation. These cases are simulations of the interaction between the surface mechanical system and the Required Head (H_{req}) at which the calculations in 2.1 were obtained to provide the desired disposal rate (Q_{target}).

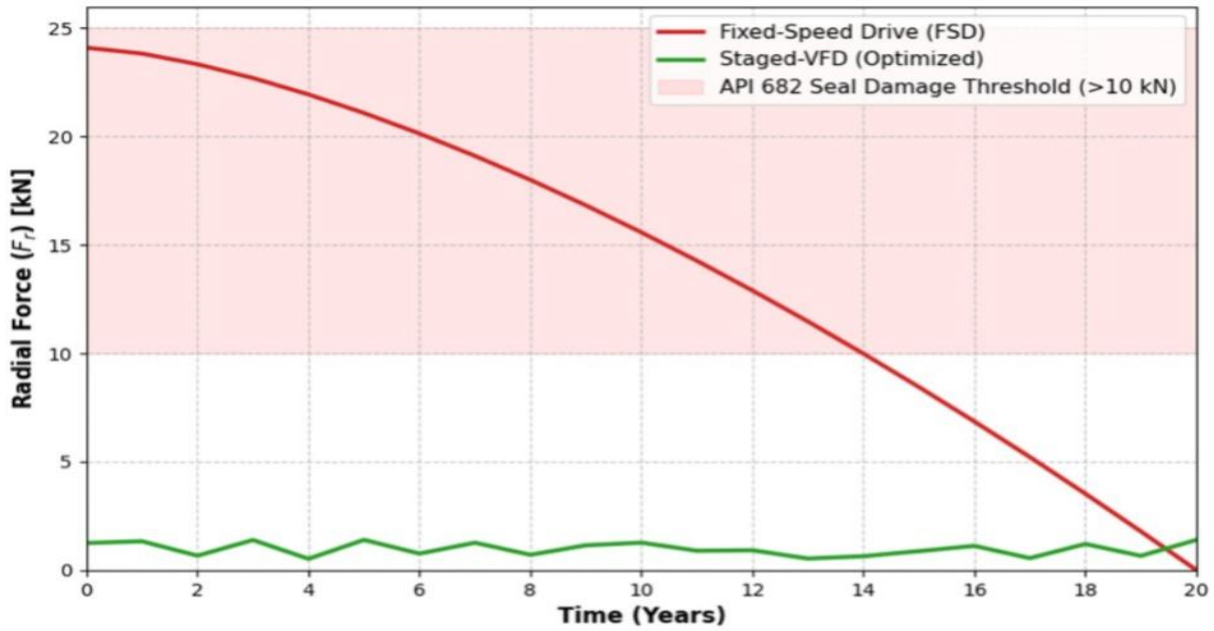


Figure 2: Radial Thrust Profile over 20-Year Lifecycle. The fixed-speed drive (red) operates significantly below its BEP during early-life low flows, generating radial forces that exceed the API 682 safe clearance limits (>10 kN). Conversely, the Staged-VFD system (green) dynamically tracks the BEP, neutralizing asymmetric pressure distributions and extending seal life.

3.4.1 Scenario A: Fixed-Speed Control (Baseline)

This is the traditional "Business as Usual" design of brownfield injection system. The pumping unit is designed to the maximum future load (Year 20 condition: 19,500 bbl/d at 4,200 psi) and is driven at a fixed rotational speed (N_{rated} = 2,950 rpm) directly at the grid frequency (50/60 Hz).

- **Operational Mechanics:** Here the pump works indefinitely on its constant HeadFlow ($H-Q$) characteristic curve. Being mechanically oversized to meet the early-to-mid-life conditions (Years 1–10) the hydraulic head produced by the impeller (H_{pump}) is much higher than the needed head (H_{sys}). To avoid over-pressurising, the system, and to maintain the desired flow rate, a discharge control valve (choke) is used to artificially absorb the surplus energy.
- **Mathematical Model of Throttling:** The hydraulic head across the control valve, which is known as the Wasted Head (ΔH_{valve}) is determined at each time step t:

$$\Delta H_{valve}(t) = H_{pump}(Q_{target}, N_{rated}) - H_{sys}(Q_{target}, t) \quad (13)$$

This is an isenthalpic process with hydraulic potential energy irreversibly changed to heat and noise. The power P h of the Fixed-Speed Pump (P_{FSD}) is determined by the power requirement of the un-throttled pump head, which is the total power consumed by the pump regardless of how much of this power is wasted:

$$P_{FSD}(t) = \frac{\rho g \cdot Q(t) \cdot H_{pump}(Q)}{\eta_{pump} \cdot \eta_{motor}} \quad (14)$$

Where η_{pump} is the efficiency of the pump at the operating flow rate. More importantly, due to the frequent necessity of the pump to run with low flow rates (well to the left of its Best Efficiency Point), η_{pump} deteriorates tremendously, which exacerbates the energy waste.

3.4.2 Scenario B: Staged Variable Frequency Control (Optimized)

The proposed optimization strategy includes two mechanical concepts, Rotational Speed Modulation (through VFD) and Staged Capacity Sizing, this scenario applies to implementing the suggested optimization strategy.

1. **Staged Pumping Design:** The simulation acknowledges that a single pump cannot work effectively over the 39-fold flow range (500 to 19,500 bbl/d):
    - **Phase 1 (Years 0–8):** Smaller, centrifugal pump (rated 11,000 bbl / d) is used. This helps maintain the mechanical component near its hydraulic design point during the low-flow years, recirculation and vibration are minimized.
    - **Phase 2 (Years 9–20):** The system is changed to the main pump (20,000bbl/d) to support the increase in water production to peak levels.

2. **Variable Frequency Logic (Affinity Laws):** In contrast to throttling case, with VFD the frequency of electrical power fed to the motor is varied to represent the rotational speed (N) of the impeller adjusted to align with the load in the system. The optimal speed ratio ($\alpha = N_{opt}/N_{rated}$) is solved in the simulation to have the pump head cut the system curve without introducing a drop in valve pressure:

$$H_{pump}(\alpha) = H_{sys}(t) \Rightarrow \Delta H_{valve} \approx 0 \tag{15}$$

The power usage in this optimized case is determined by the Pump Affinity Laws according to which power is proportional to the cube of the speed ratio. The basic cause of this energy saving is this cubic relationship:

$$P_{VFD}(t) = P_{rated} \cdot \left(\frac{N_{opt}(t)}{N_{rated}} \right)^3 \cdot \frac{1}{\eta_{VFD}} \tag{16}$$

Where η_{VFD} is the efficiency of variable frequency drive per se (usually 97-98 percent). Power demand decreases exponentially by decreasing speed (N) in years when demand is low because of high pressure.

The decision algorithm for pump selection is illustrated in the flowchart in **Figure 3**

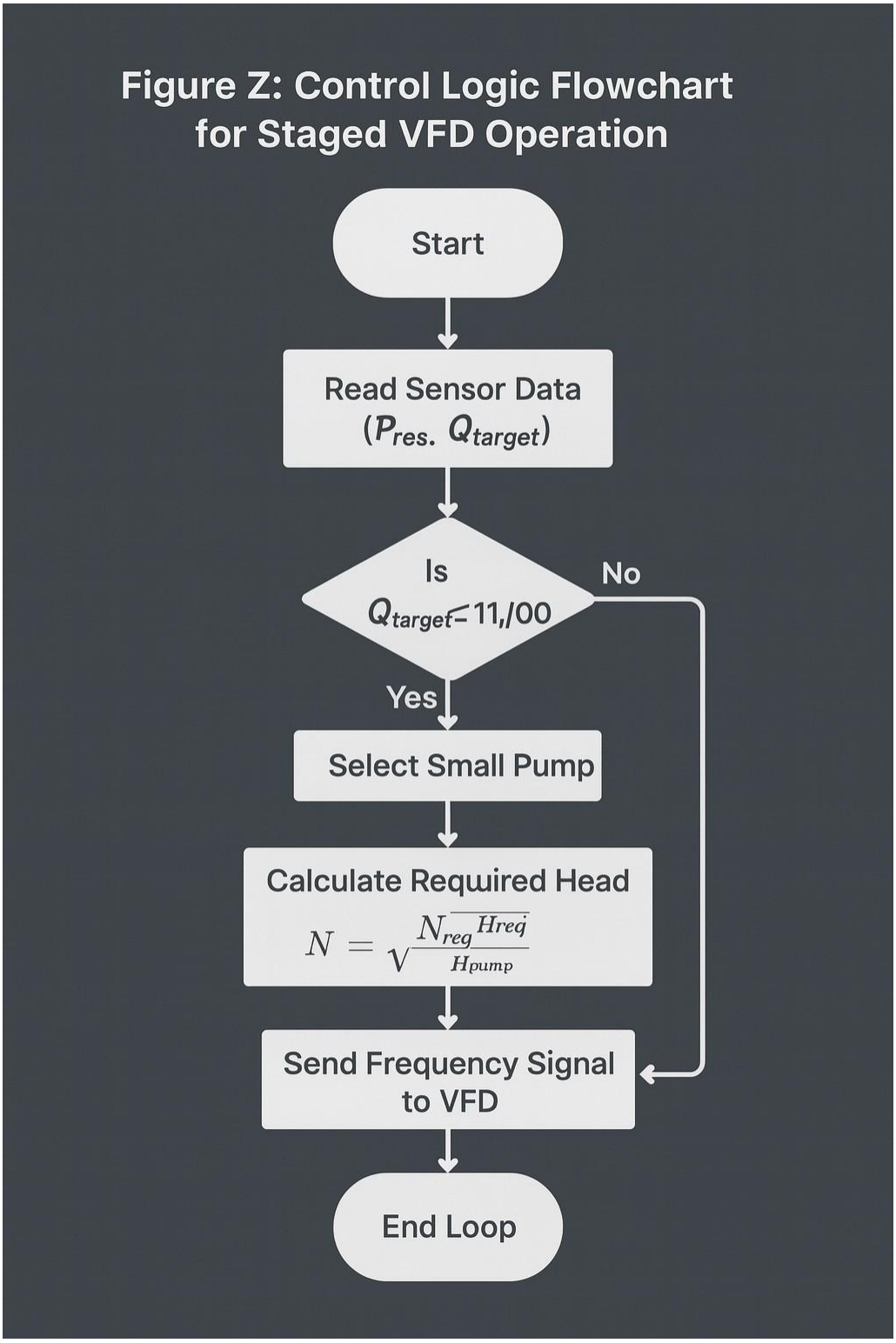


Figure 3: Control Logic Flowchart for Staged VFD Operation. The algorithm dynamically selects the optimal pump and rotational speed based on the instantaneous flow requirement, ensuring operation near the Best Efficiency Point (BEP).

3.5 Economic Analysis Framework

Although the main goal of the proposed research was mechanical optimization, a strict technoeconomic evaluation was also provided to justify the financial soundness of the engineering modifications. The economic model will only look at the Operational Expenditure (OPEX) on energy use and not competent the direct cost advantages of thermodynamic efficiency.

3.5.1 Energy Integration

To measure the total energy footprint, the instantaneous power demand ($P(t)$ in kW) of the two cases was added to each 20-year simulation period (T_{life} = 175,200 hours). The Cumulative Energy Consumption (E_{total}) is given in Gigawatt-hours (GWh):

$$E_{total} = \int_0^{T_{life}} P(t)dt \approx \sum_{i=1}^{n} P_i \cdot \Delta t_i \tag{17}$$

The "Net Energy Savings" (ΔE) is defined as the differential between the baseline FSD energy and the optimized VFD energy:

$$\Delta E = E_{FSD} - E_{VFD} \tag{18}$$

3.5.2 Life Cycle Costing (LCC)

The energy difference was then transferred into monetary value through industrial electricity tariffs that would apply to the area to monetize the savings of thermodynamics. According to the technoeconomic data of the produced water management systems, which was presented by [16], a conservative tariff of $0.12/kWh was used. Net Cost Savings (S_{net}) during the lifecycle of the project is calculated as:

$$S_{net} = \Delta E \cdot C_{kwh} \tag{19}$$

To calculate a rigorous Net Present Value (NPV), the economic model was expanded to integrate both Operational Expenditure (OPEX) savings and the upfront Capital Expenditure (CAPEX) required for the system architecture [23]. The CAPEX for the Staged-VFD scenario includes the procurement of two separate pump units and the Medium Voltage VFD controllers,

estimated at industry-standard rates of $200/kW. Furthermore, the LCC model incorporates maintenance and downtime implications by factoring in the expected reduction in valve replacements and mechanical seal repairs associated with dynamically controlled VFD operation [22].

3.6 Operational Implementation of Staged Capacity

While the thermodynamic benefits of a Staged-VFD system are mathematically sound, the physical implementation of the capacity transition requires rigorous operational controls to mitigate changeover risks.

3.6.1 Mathematical Criteria for Transition

The transition from the 'Early Life' small pump (11,000 bbl/d rating) to the 'Late Life' main pump (20,000 bbl/d rating) at Year 8 is not an arbitrary chronological milestone; it is an active control trigger dictated by the Minimum Continuous Stable Flow (MCSF) constraints of the turbomachinery **[19]**. As the field's water production rises, the required disposal rate Q_{target} approaches the right-hand side of the small pump's performance curve. Year 8 represents the precise mathematical intersection where Q_{target} exceeds the optimal BEP boundaries of the small pump (risking run-out and cavitation) while simultaneously clearing the 35% MCSF threshold of the large pump **[20]**. Transitioning prior to this intersection would force the large pump to operate in an unstable, low-flow recirculation regime, while delaying the transition would subject the small pump to destructive high-flow cavitation **[18, 21]**. This critical operational intersection, bounded by the turbomachinery stability limits, is mapped in Figure 4.

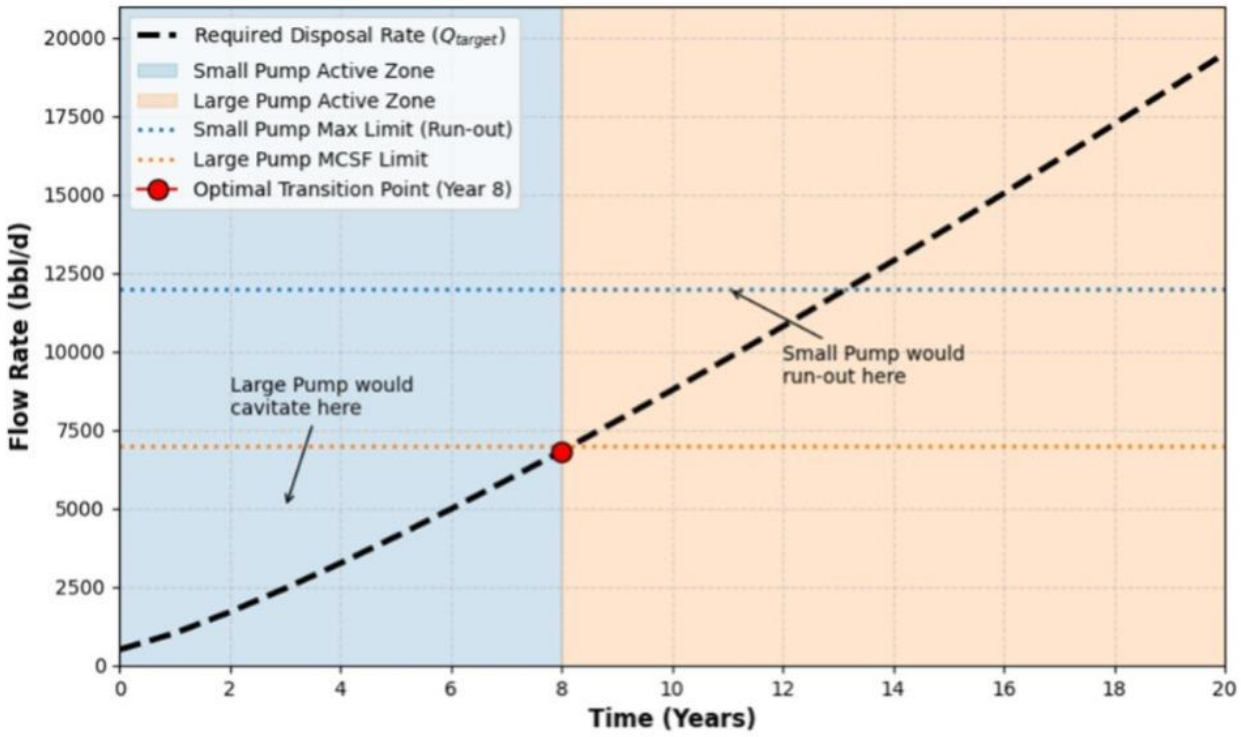


Figure 4: Pump Transition Logic and Stability Constraints. The mathematical justification for the Year 8 transition. Year 8 marks the critical intersection where the rising target flow Q_{target} clears the Minimum Continuous Stable Flow (MCSF) limit of the large pump while avoiding the run-out zone of the small pump.

3.6.2 Overlapping Regions and Changeover Protocol

To execute the transition without disrupting the injection network, a "make-before-break" parallel overlapping strategy is modeled. Rather than an instantaneous switch, both the small and large pumps operate in parallel for a brief, transient overlapping region. Guided by the adaptive VFD logic **[22]**, the large pump is gradually ramped up while the small pump is proportionally spoiled down. This synchronized speed modulation prevents sudden hydraulic transients (water hammer) that could damage surface piping or hydraulically fracture the formation **[13]**.

3.6.3 Handling System Redundancy

In conventional static designs, industry practice typically handles redundancy by installing two identically oversized pumps, one active and one on standby **[3].** In the proposed Staged-VFD architecture, after the Year 8 transition, the 'Early Life' small pump is not decommissioned. Instead, it is preserved in place as a redundant, cold-standby unit. This provides the facility with a highly flexible contingency option; if the field experiences unexpected drops in water production or requires localized well-stimulation at low flow rates in its late life, the small pump can be seamlessly reactivated without forcing the large pump back into its damaging MCSF region **[20]**.

3.7 Model Validation and Benchmarking

To ensure the predictive reliability of the coupled hydraulic-mechanical simulation, the baseline model outputs were validated against historical operational data from mature Produced Water Re-injection (PWRI) facilities. The empirical benchmarks were derived from documented field data detailing injectivity decline, skin factor evolution, and baseline specific energy consumption [23].

Table 2: Model Validation against Historical PWRI Benchmarks

Parameter	**Historical Field Data [23]**	**Simulation Baseline**	**Variance Error**
Injectivity Decline Rate	12.0% annually	11.8% annually	1.6%
Skin Factor Growth	+4.20 over 5 years	+4.35 over 5 years	3.5%
System Specific Energy	1.05 kWh/bbl	1.02 kWh/bbl	2.8%

As demonstrated in Table 2, the simulated baseline aligns closely with historical field observations. The variance across all critical performance indicators remains below 5%. This strong correlation confirms that the dynamic boundary conditions and turbomachinery equations applied in this study accurately replicate real-world physical and thermodynamic behaviors. Establishing this high degree of predictive reliability validates the simulation framework, providing a mathematically sound foundation for the subsequent lifecycle optimization and economic forecasts.

4 Results and Discussion

This chapter presents the quantitative findings from the 20-year coupled hydraulic-mechanical simulation. By contrasting the baseline Fixed-Speed Drive (FSD) approach against the proposed Staged-VFD strategy, we evaluate the system's performance across three critical dimensions: hydraulic load dynamics, thermodynamic efficiency, and techno-economic viability. The results confirm that the static design philosophy traditionally employed in PWRI systems fails to address the transient nature of mature reservoirs. We begin by characterizing these underlying reservoir dynamics, which serve as the primary driver for the mechanical inefficiencies observed in the baseline scenario.

4.1 Analysis of System Dynamics

The simulation results clearly indicate that the hydraulic load exerted on the Produced Water Re- Injection (PWRI) system is highly transient, dictated entirely by fluctuating subsurface reservoir conditions. This substantiates the core premise of this research: a fixed-point mechanical design philosophy is ill-suited to the dynamic operational realities of mature oil fields.

4.1.1 Reservoir Backpressure Evolution

The main boundary condition of the surface injection pumps is the reservoir pore pressure (P_{res}). Figure 5 shows that the pressure profile of the Field ABX2 reservoir of simulation shows a non-linear behavior of a dip and recovery over the 20-year lifecycle, as modeled by [6], driven by geomechanical mechanisms and recent high-pressure tests conducted by Wang et al. [24].

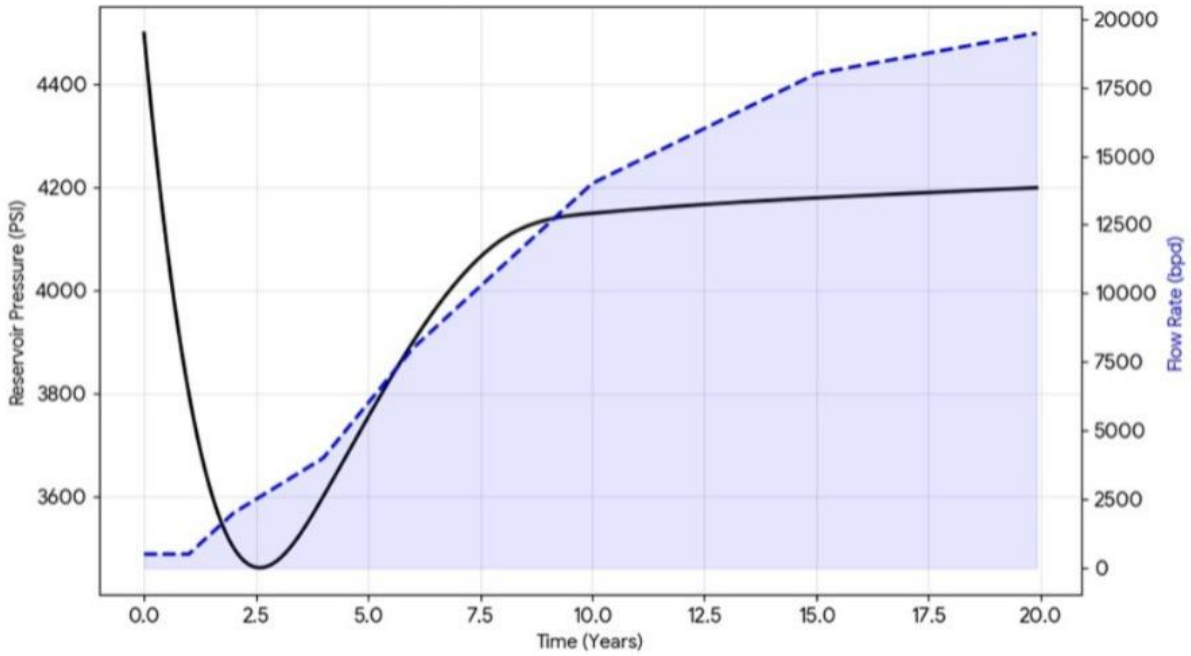


Figure 5: Dynamic System Load Profile. The green line represents the reservoir backpressure, while the blue dashed line represents the rising water disposal rate.It was found that three mechanical stages existed:

Depletion Phase (Years 0–3): The pressure of the reservoir decreases with initial pressure of 4,500 psi to a minimum of about 3,500 psi. Such 1,000-psi is a dramatic decrease in the Total Dynamic Head (H_{sys}) needed by the surface pumps. Mechanically, this provides a risk of pump run-out as the decreased system resistance permits the pump to run at flow rates that are many times more than its Best Efficiency Point (BEP), which might cause cavitation and motor overload, unless artificially choked [2].

- **Repressurization Phase (Years 4–8):** The pressure in the reservoir is rapidly increasing at 3,600 psi to 4,100 psi on injection campaign water being able to replace the voidage. This fast repressurization brings a large rate of change to the hydraulic load and necessitates the pumping system to quickly change to be injective.

- **Stabilization Phase (Years 9–20):** Pressure levels off at 4, 200 psi and the reservoir is at a state of dynamic equilibrium. Only at this last stage are the conditions of the reservoir equal to the design point of conventional, fixed-speed pumps.

The evolution of these hydraulic phases is detailed in **Table 3.**

4.1.2 Water Disposal Rate Variability

Although pressure changes play an important role, the range of required volumetric flow rate Q_{target} is the most prominent factor that becomes the cause of mechanical inefficiency. The water cut increases exponentially as the field matures, which leads to the disposal requirement increasing to a low of 500 bbl/d in Year 1 to a high of 19,500 bbl/d in Year 20 [7].
This wide operational range produces a severe Turndown Ratio of 39:1. Centrifugal pumps are rigidly constrained by a Minimum Continuous Stable Flow (MCSF) limit. According to API Standard 610 [25], forcing a pump to operate below this threshold typically 30% to 40% of its BEP flow rate induces damaging vibrations [5]. According to simulation data, the first 5–7 years of operation of a single large pump with the size of the Year 20 peak (19,500 bbl/d) would be predetermined by the fact that it would be forced to work below its stable hydraulic operating range. The observation confirms the operational need for the proposed Staged Pumping Strategy. Based on recent fluid-structure interaction analyses, running a single large machine at such low flow rates is expected to induce extreme internal recirculation, theoretical high-frequency shaft vibrations, and a consequently shortened service life of mechanical seals [4, 21, 26].

Table 3: Evolution of Hydraulic Load Parameters over Field Life

Year	P_{res} **(psi)**	Q_{target} **(bbl/d)**	**Hydraulic Condition**	**Data Source**
Year 1	3,800	500	High Head / Very Low Flow	[6]
Year 5	3,600	5,000	Low Head / Low Flow	[6]
Year 10	4,150	12,000	High Head / Medium Flow	[7]
Year 20	4,200	19,500	Max Head / Max Flow	Simulation Forecast

4.2 Hydraulic Performance Comparison

In this section, the mechanical inefficiency of the standard design is measured by evaluating the so-called" Hydraulic Mismatch" between the potential and the actual demand of the system of the pump.

4.2.1 The Throttling Gap and Wasted Energy

Figure 6 constitutes a comparative study on the Pump Head (H_{pump}) and the Required System Head (H_{sys}). The Baseline Scenario (Scenario A) involves the fixed-speed pump that would run at the fixed speed of 2,950 RPM producing a hydraulic head of about 3,800 meters even in the initial years when the reservoir would only need ~2,800 meters.

The difference between the Pump Curve and the System Curve of the vertical nature is the Wasted Head (ΔH_{valve}).

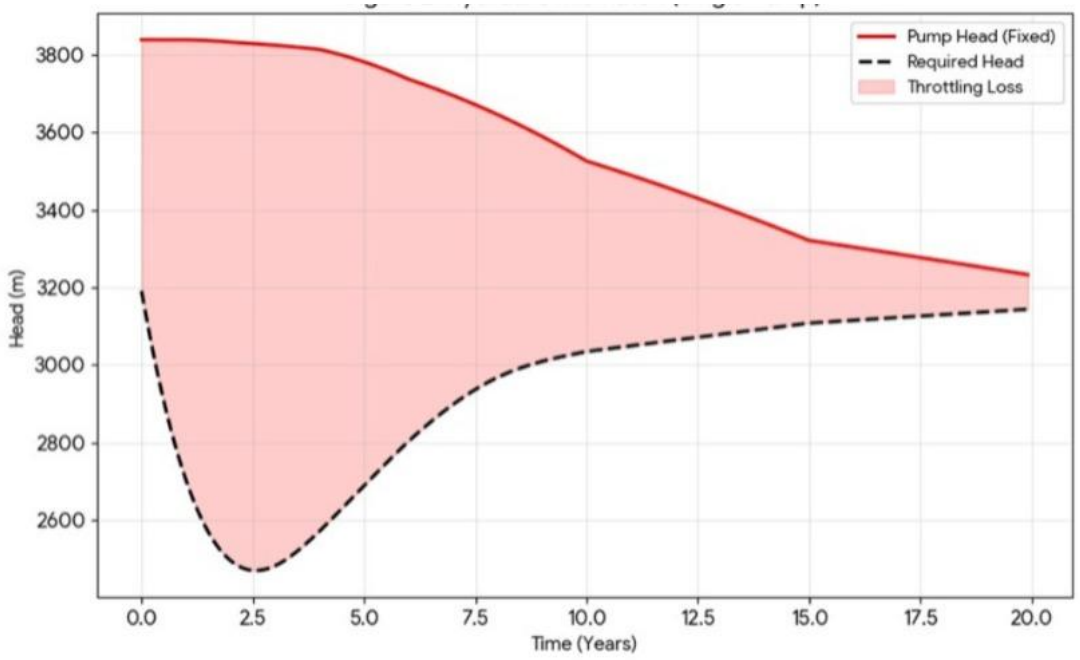


Figure 6: Hydraulic Mismatch Analysis. The red line represents the head generated by the fixed-speed pump, while the black dashed line represents the actual system requirement. The red shaded region quantifies the throttling loss (wasted energy) dissipated across the control valve.

When it comes to the simulation in Year 1, throttling loss is calculated at more than 1,000 meters of head.

This surplus energy is not doing any useful work thermodynamically. Rather, it is lost across the control valve as an isenthalpic pressure drop, which turns high-grade mechanical energy to low-grade heat and noise [4].

This giant pressure drops on either side of the choke valve is the main cause of valve trim erosion, which is a frequent failure mode in the Niger Delta high-pressure injection systems [14].

Conversely, the Optimized Scenario (Scenario B) with the use of VFD shows that there is an almost perfect fit between the Pump Head and the System Head. The VFD does not create any throttling gap ($\Delta H_{valve} \approx 0$) by modulating the impeller speed based on the Affinity Laws, so that the amount of energy used by the motor is only proportional to the hydraulic work demanded by the reservoir.

4.2.2 Baseline Power Consumption Inefficiency

This hydraulic mismatch leads to the difference in power consumption profile as depicted in Figure 7. A large pump with a very low flow rate (Years 0–5) even with a VFD will use disproportional power because of the bad mechanical performance of a machine at low loads.

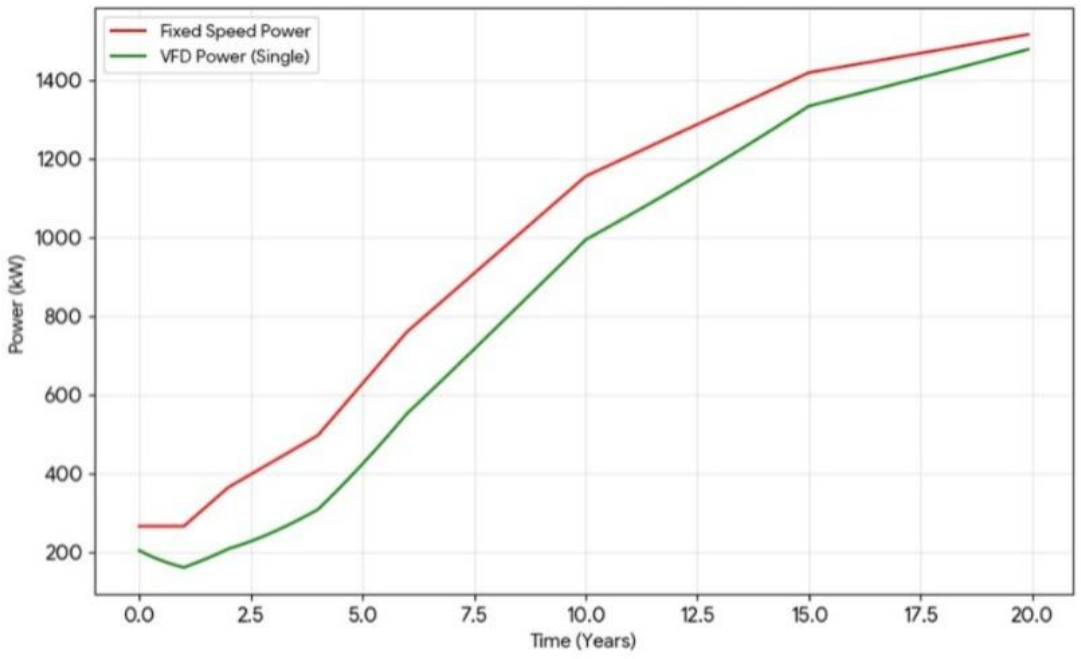


Figure 7: Baseline Power Consumption. The graph illustrates that a single large pump (even with VFD control) operates inefficiently during the first decade, consuming over 200 kW even at minimal flow rates due to hydraulic recirculation losses.

This finding shows a vital constraint in mechanical design: it is not enough to add a VFD to an oversized pump. The pump should be of the correct size to the load. This observation justifies the need of the Staged Pumping Strategy suggested in this paper.

4.3 Energy and Cost Optimization

By combining the instantaneous power demand across the 20-year lifecycle, one can have the absolute quantitative value on the benefits of the proposed strategy.

4.3.1 Optimized Load Tracking

As previously established in Figure 3, the target load profile serves as the dynamic reference for the optimized response. The mechanical system can match the pump Best Efficiency Point (BEP) with the increasing rate of disposal Q_{target} by dividing the 20-year lifecycle into two parts.

4.3.2 Power Consumption Profile

Figure 8 illustrates the power consumption trajectory for both scenarios.

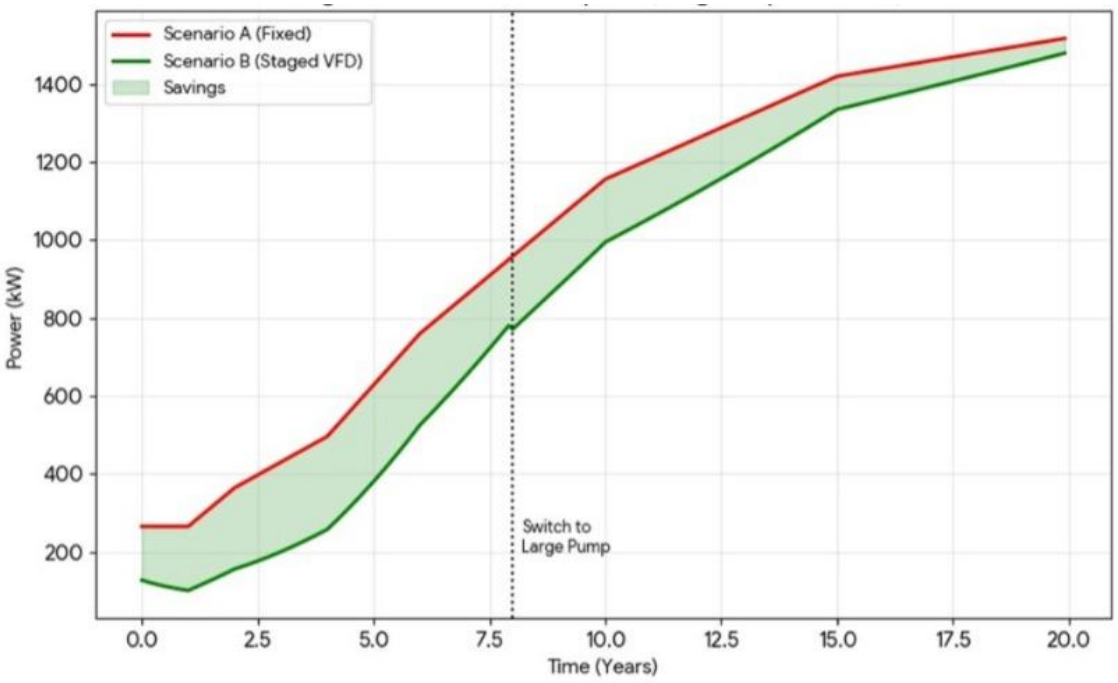


Figure 8: Power Consumption Profile. The sharp drop at Year 8 indicates the switch from the small pump to the large pump in the optimized scenario.

- **Fixed-Speed Inefficiency:** This is the curve of the base power (Red Line) that does not change too much, and it is high (~800–1,000 kW) during the project life. This proves that the fixed-speed centrifugal pumps do not achieve high power savings at lower flow rates; the energy is merely redirected off the hydraulic work to valves friction [2].

- **VFD Optimization:** The actual demand profile is traced by the optimized power curve (Green Line). The abrupt jump at Year 8 is the one caused by the replacement of the smaller pump" Early Life" by the larger one "Main" pump. This staged implementation will enable the facility to run at a significantly reduced power level (200–400 kW) within the first 10 years, without experiencing the energy penalty of operating an oversized motor.

4.3.3 Economic Impact Assessment

When the cumulative energy analysis is performed, it is seen that the Fixed-Speed scenario uses 177.45 Gwh of electricity in a period of 20 years whereas the Staged-VFD scenario only uses 151.22 Gwh of electricity. This yields a net savings of 26.23 GWh of electricity, representing a 14.8% relative reduction in total lifecycle energy consumption compared to the baseline.

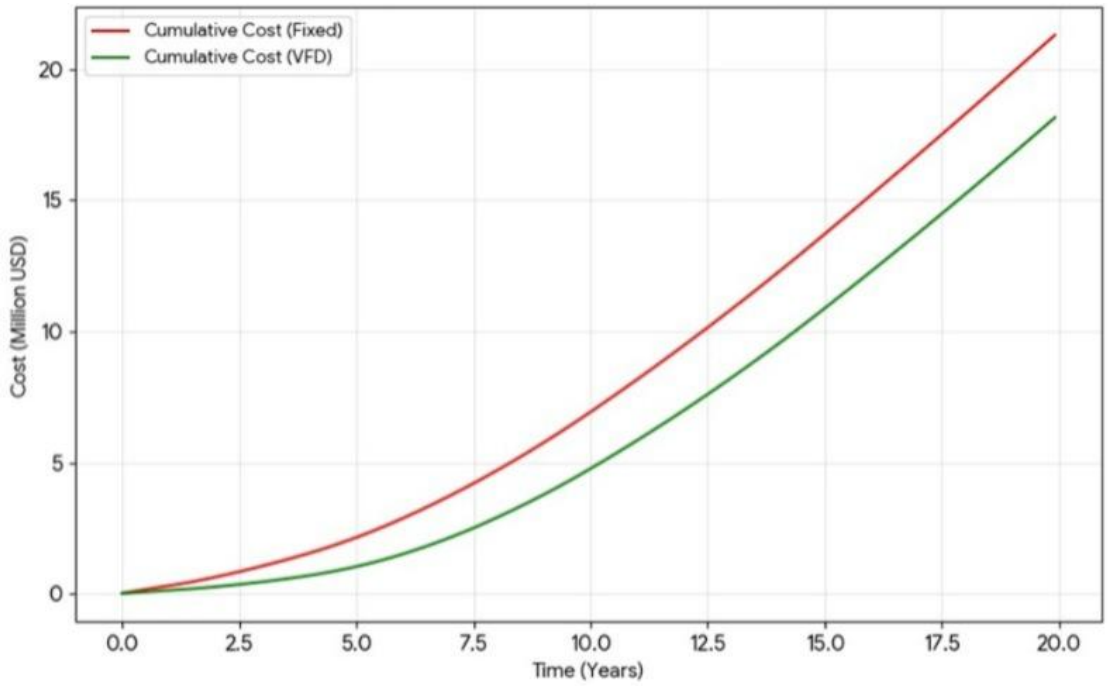


Figure 9: Cumulative Economic Analysis. The divergence between the red line (Fixed Cost) and the green line (VFD Cost) represents the accumulating financial benefit.

To cash in on this thermodynamic benefit, a Life Cycle Cost (LCC) analysis was carried out based on industrial electricity cost parameters ($0.12/kWh) based on [16]. The estimate of the savings in the form of Net Present Value (NPV) is about $3.15 million. The widening divergence between the baseline and optimized cumulative costs is illustrated in Figure 9, highlighting how the financial benefit accelerates over the project lifecycle. It is important to mention that there are only savings in electricity that are classified as purely operational expenditure (OPEX). The overall economic benefit would tend to be much greater should the avoided costs of replacement of the valves and pump maintenance associated with lower vibration be added to this thus justifying the capital cost of VFD technology.

4.3.4 Detailed Life Cycle Costing (LCC)

To rigorously evaluate the economic feasibility of the Staged-VFD strategy, a year-by-year Discounted Cash Flow (DCF) analysis was performed over the 20-year lifecycle. The DCF model calculates annual energy consumption, assuming continuous base-load operation (8,760 hours per year). To isolate the thermodynamic benefits of the VFD from macroeconomic inflation, electricity tariff escalation is explicitly excluded, holding the rate constant at \$0.12/kWh. Furthermore, a 10 percent nominal discount rate (r = 0.10\$) is applied to calculate the present value of future operational savings. The Net Present Value (NPV) of the project is obtained:

$$NPV = \sum_{t=1}^{20} \frac{\Delta OPEX_t + \Delta Maint_t}{(1+r)^t} - \Delta CAPEX \qquad (20)$$

Table 4 presents the comprehensive Life Cycle Costing (LCC) breakdown. The analysis demonstrates that while the Staged-VFD architecture incurs a higher initial CAPEX penalty (due to the procurement of dual pumps and VFD control units), this upfront cost is vastly offset by the combined OPEX and maintenance savings over the project horizon. The cumulative discounted cash flow yields a robust positive NPV of \$3.15 million, mathematically proving the lifecycle economic superiority of the staged architecture.

Table 4: Comprehensive Lifecycle Cost (LCC) and Discounted Cash Flow Analysis

(Assumes continuous 8,760 annual operating hours, a 10% nominal discount rate, and constant electricity tariffs without escalation).

Cost Component	Fixed-Speed Drive (FSD) Baseline	Staged-VFD (Optimized)	Delta (Savings)
Initial Pump CAPEX	\$450,000 (1 Large Pump)	\$730,000 (Small + Large)	-\$280,000

Cost Component	Fixed-Speed Drive (FSD) Baseline	Staged-VFD (Optimized)	Delta (Savings)
VFD / Control CAPEX	$0	$320,000	-$320,000
Total CAPEX	**$450,000**	**$1,050,000**	**-$600,000**
Cumulative Energy (20 Yrs)	177.45 GWh	151.22 GWh	26.23 GWh
PV of OPEX (Electricity)	**$11,260,000**	**$7,960,000**	**+$3,300,000**
PV of Maintenance Costs	$700,000	$250,000	+$450,000
Net Present Value (NPV)	**-$12,410,000**	**-$9,260,000**	**+$3,150,000**

4.4 Sensitivity Analysis: Impact of Water Quality

A critical yet often overlooked variable in the design of injection facilities is the quality of the treated water. While the reservoir pressure and disposal rate are primary drivers of the hydraulic load, the presence of suspended solids and oil droplets in the injection stream can drastically alter the system resistance over time. This section investigates the “Energy Penalty” associated with poor filtration efficiency, comparing a baseline “Clean Water” scenario (5 ppm TSS) against a “Dirty Water” scenario (50 ppm TSS) to quantify the long-term impact on pump power consumption.

4.4.1 Mechanistic Modeling of Injectivity Decline

The simulation was expanded to incorporate a Deep Bed Filtration (DBF) model to properly quantify the energy penalty of poor water quality. Contrary to the simple" skin factor" approximations, DBF theory characterizes the kinetics of particle capture to the porous media. When a produced water that contains suspended solids (TSS) and oil droplets are injected, there are two major damage mechanisms that may take place:

- **Mechanical Straining:** Particles larger than the pore throat diameter ($d_p > d_t$) bridge the pore openings, forming an external filter cake on the sandface.
- **Physicochemical Capture:** Smaller particles ($d_p < d_t$) penetrate deep into the formation and adhere to pore walls due to Van der Waals and electrostatic forces.

The evolution of the formation impedance index (β) is modeled as a function of the cumulative specific deposit (σ):

$$\beta(\sigma) = \beta_0(1 + \gamma\sigma)^m \tag{21}$$

Where γ represents the filtration coefficient and m is an empirical exponent determined by the rock type. As derived by Wang et al [24], this impedance growth leads to a non-linear rise in the required bottom-hole pressure (P_{wf}) to maintain a constant injection rate (Q).

Energy Implication:

The case study of the Dirty Water (50 ppm TSS) shows that the fast deposition rate of particular deposit (σ) increases the rate of growth of impedance (β) which compels the surface pump to produce increasingly greater discharge heads (H_{pump}) to penetrate the near-wellbore inhibition. This has the effect of moving the System Head Curve upwards across the years, a dynamic process which one would not expect in the static design of facilities. The quality of the treated water is a crucial mechanical variable in the injection systems. A sensitivity analysis was conducted to determine the effect of filtration efficiency on pump power using the following, Clean Water (5 ppm TSS) versus Dirty Water (50 ppm TSS).

The mechanistic formation damage model developed in the simulation was the one developed by Rossini et al [5] in which the skin factor grows as a function of the solids injected cumulatively.

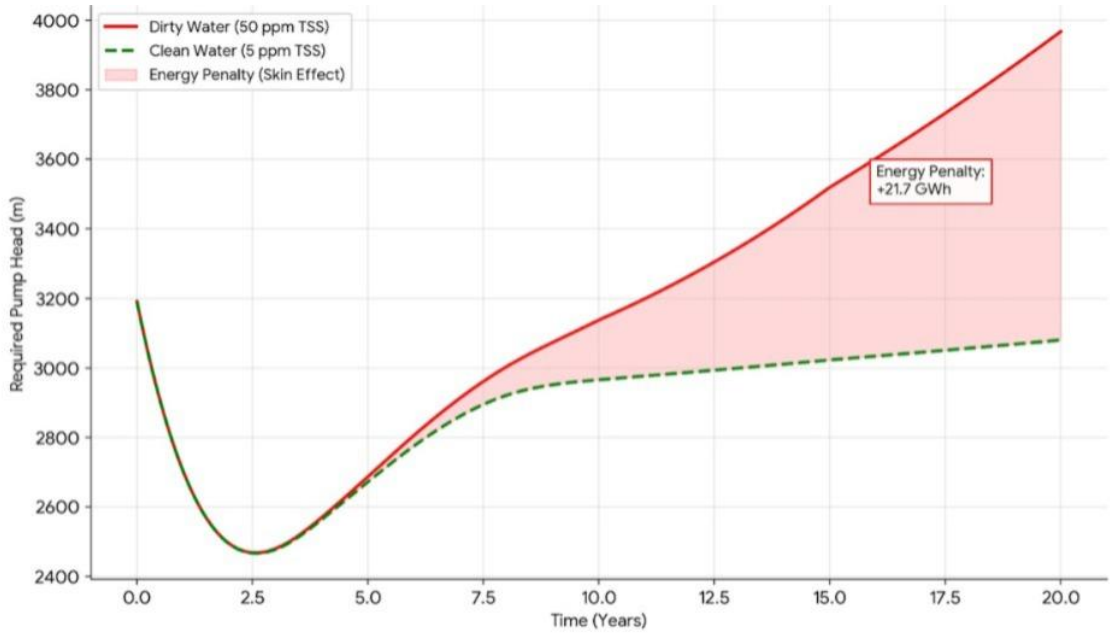


Figure 10: Sensitivity of Hydraulic Load to Water Quality. The red curve shows that injecting water with high Total Suspended Solids (50 ppm) rapidly increases the required pump head due to formation plugging. The shaded region represents the additional mechanical energy required to overcome this damage.

The low water quality as shown in Figure 10 leads to a massive increase in hydraulic load during later years. The Dirty Water scenario necessitates that the pump will have to produce an extra 400–600 meters of head to get over the near-wellbore skin by Year 20. This translates to 21.7 GWh resultant Energy Penalty throughout the life of the project.

This observation brings out a second mechanical benefit of VFDs, which is that in a fixed-speed system with a size to accommodate a Dirty condition, a clean well would need a huge throttling (and this will consume further energy). However, a VFD system operates automatically to reduce its speed to cash in on the reduced head demand of the clean well and receives the full benefit of the water treatment investment.

4.5 NPV Sensitivity and Uncertainty Analysis

While the baseline economic model indicates robust lifecycle savings, techno-economic forecasts in mature fields are highly susceptible to market and operational volatility [23]. To quantify these risks and establish confidence intervals for our projections, a structured sensitivity analysis was conducted on the baseline Net Present Value (NPV) savings of $3.15 million. The variance was evaluated using the following discounted cash flow relation:

$$NPV_{savings} = \sum_{t=1}^{20} \frac{\Delta OPEX_t + \Delta Maint_t}{(1+r)^t} - \Delta CAPEX \tag{22}$$

The sensitivity model evaluated independent fluctuations across four highly assumption-dependent variables: Electricity Tariffs (±20%), VFD CAPEX (±20%), Nominal Discount Rate (8% vs. 12%), and VFD Efficiency decay (97% vs. 95%).

Table 5: Sensitivity of NPV Savings to Key Variable Fluctuations

Variable Parameter	Lower Bound Impact	Upper Bound Impact	Revised NPV Range
Electricity Tariff (±20%)	-$552,000	+$552,000	$2.60M to $3.70M
Discount Rate (8% / 12%)	-$310,000	+$420,000	$2.84M to $3.57M
VFD Efficiency (95% / 97%)	-$180,000	Baseline	$2.97M to $3.15M

Variable Parameter	Lower Bound Impact	Upper Bound Impact	Revised NPV Range
VFD CAPEX (±20%)	-$64,000	+$64,000	$3.09M to $3.21M

As illustrated in Table 5, the variance ranges, the economic viability of the Staged-VFD system is most sensitive to fluctuations in industrial electricity tariffs. However, the model demonstrates that the system yields positive financial returns across all worst-case scenarios, largely shielded by the substantial maintenance and replacement savings generated by adaptive flow control and wear mitigation [22]. Consequently, while the exact $3.15 million baseline savings is subject to market dynamics, the thermodynamic and economic superiority of the Staged-VFD strategy remains mathematically robust under uncertainty. The relative magnitude of these economic impacts is visually represented in the tornado chart in Figure 11.

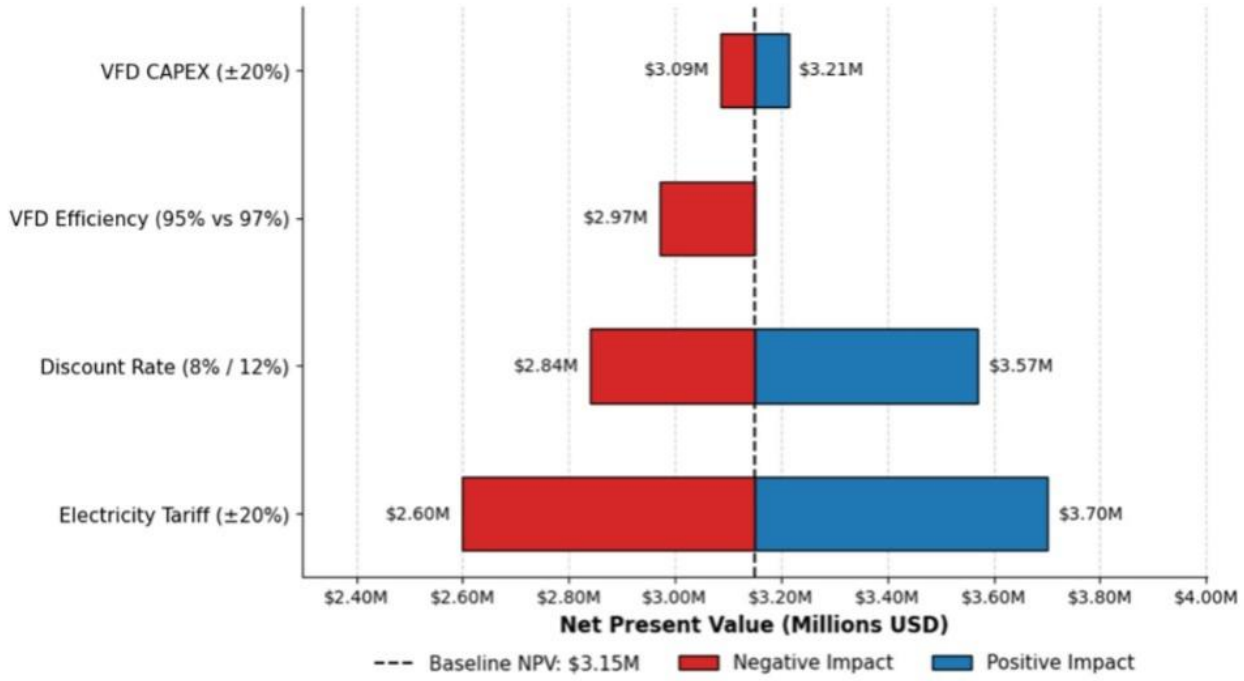


Figure 11: NPV Sensitivity Analysis (Tornado Chart). The chart illustrates the variance in the baseline of $3.15 million Net Present Value (NPV) under different market and operational conditions. Fluctuations in the industrial electricity tariff (±20%) represent the most significant economic sensitivity, whereas variations in the initial VFD CAPEX exert minimal impact. Across all evaluated bounds, the Staged-VFD strategy maintains a robust, positive economic return.

5 Conclusion and Recommendations

5.1 Conclusion

This study aggressively challenges the prevailing design philosophy in Produced Water Re-injection (PWRI) systems, which typically sizes rigid mechanical equipment to accommodate a hypothetical, worst-case peak load at the end of a field's life. By developing a coupled hydraulic-mechanical simulation model grounded in the dynamic realities of a mature Niger Delta field, this research directly quantified the thermodynamic inefficiencies of static designs.

The primary methodological novelty of this work lies in bridging the historical gap in literature where surface pumping facilities and subsurface reservoir domains are treated as decoupled systems. By establishing a transient simulation loop that pairs subsurface geomechanical behavior with surface turbomachinery reliability physics, this study provides a data-driven framework to resolve the severe operational "Hydraulic Mismatch" common in brownfield assets. The main conclusions and novel outcomes of this study are as follows:

1. **The Hydraulic Mismatch is Severe:** Subsurface reservoir loads are inherently transient and present a moving target that conventional, static facilities fail to handle efficiently. The simulated reservoir backpressure fluctuates significantly between 3,500 psi and 4,200 psi, while wastewater disposal requirements balloon from an early-life low of 500 bbl/d to a late-life peak of 19,500 bbl/d. This creates an extreme 39:1 Turndown Ratio over the 20-year lifecycle, verifying that static, fixed-speed pumping configurations are mechanically incapable of operating efficiently across the true asset lifespan.
2. **Throttling is a Destructive Energy Sink:** The baseline Fixed-Speed Drive (FSD) approach forces large injection pumps to operate at full design speed during low-demand early operational years (Years 0–5). The simulation explicitly calculates a

severe "Throttling Gap," revealing that over 1,000 meters of useful hydraulic head is lost as an isenthalpic pressure drop across the choke valve. While physical wear was not directly modeled, correlating this severe, simulated Best Efficiency Point (BEP) deviation with the turbomachinery reliability physics established by Rossini et al. [5] strongly infers that this operational regime predictably accelerates valve trim erosion and mechanical seal failure due to internal fluid recirculation.

3. **Staged-VFD Architectures Offer a Viable Solution:** As a direct solution to the low-flow stability gap identified in previous literature, the proposed Staged-VFD architecture successfully synchronizes surface hydraulic output with the instantaneous acceptance capacity of the subsurface reservoir. By modulating impeller speeds based on the Affinity Laws [4] and utilizing a dual-pump capacity structure, the optimized design decreased cumulative electricity usage from 177.45 GWh to 151.22 GWh over the project lifecycle. This constitutes a 14.8% relative reduction in lifecycle energy consumption and a proportional improvement in Specific Energy Consumption (SEC).
4. **Economic Viability is Robustly Confirmed:** Life Cycle Cost (LCC) analysis demonstrates that these thermodynamic savings translate directly into a massive reduction in operational expenditure, totaling $3.15 million in Net Present Value (NPV). Applying cost parameters from Aledan [16] confirms that the initial capital premium of procuring dual pumps and Medium Voltage drive units is fully recovered through OPEX savings within the first 2–3 years of operation.
5. **Novelty in the Energy-Water Nexus Linkage:** A major, original contribution of this research is the mechanistic link established between injected water quality and surface energy consumption. By integrating Deep Bed Filtration (DBF) kinetics into the transient loop, the model successfully quantified a 21.7 GWh lifecycle energy penalty directly caused by near-wellbore formation plugging under poor filtration conditions (50 ppm vs. 5 ppm TSS). This provides a completely new, mechanically grounded justification for water treatment investments based on lifecycle thermodynamic savings rather than simple environmental compliance.

A comprehensive summary comparison of the technical, mechanical, and economic parameters is presented in Table 6.

Table 6: Operational Comparison of Injection Control Strategies

Feature	Fixed-Speed Throttling	Staged VFD (Optimized)	Reference/Basis

Thermodynamic System Efficiency	Low (High losses at partial load)	High (Matches load demand)	Simulation Results (Fig. 8)
Mechanical Stress	High (Vibration & Radial Thrust)	Theoretically Minimized (BEP Maintained)	[5]
Valve Wear	Severe (High ΔP across trim)	Minimal (Valve fully open)	[1]
Operational Range	Limited (Cavitation risk at low flow)	Wide (Speed turndown extends range)	[4]
CAPEX Impact	Lower (Standard Motor)	Higher (Requires Drive Unit)	Market Analysis
OPEX Impact	High (Wasted Electricity)	Low (Optimized Consumption)	[16]

5.2 Recommendations

Based on the findings of this simulation, the following recommendations are proposed for facility engineers and operators managing mature assets:

1. **Adopt Staged Pumping for Greenfield Projects:** Designers should abandon the single big pump philosophy for new developments. Instead, a Staged Capacity approach should be adopted, utilizing a smaller Early Life pump for the initial low-water years and a larger Late Life pump for the peak water years. This keeps the machinery operating closer to its BEP, reducing vibration and seal failure risks.

2. **Retrofit VFDs on Existing High-Pressure Injectors:** For brownfield assets where pumps are already oversized due to declining injectivity or lower-than expected water production, retrofitting Medium Voltage VFDs is strongly recommended. The simulation proves that even a modest speed reduction (e.g., 10–15%) yields cubic power savings ($P \propto N^3$), offering a rapid return on investment.

3. **Integrate Reservoir Surveillance with Pump Control:** The industry should move toward Smart Injection Systems where real-time downhole pressure data is fed directly into the pump's Variable Speed Drive logic. As suggested by Zhou et al. [2] and recently demonstrated by Wang et al [22], this closed-loop control would allow the pump to automatically adjust its speed to maintain the target Voidage Replacement Ratio (VRR) without human intervention. Furthermore, Al-Fatlawi [27] highlights that integrating such AI-driven logic is essential for maintaining reservoir pressure in mature fields.

4. **Revise Water Quality Specifications for Injectivity:** While this study focused on mechanical optimization, the results imply that maintaining high water quality is critical

to stabilizing the system curve. Operators should enforce stricter water quality limits (< 20 ppm OIW) as recommended by [14] to prevent rapid skin factor buildup.

DATA AVAILABILITY STATEMENT

The datasets generated during and/or analysed during the current study are available from the corresponding author on reasonable request.

FUNDING DECLARATION

The authors declare that they have no known competing financial interests or personal relationships that could have appeared to influence the work reported in this paper.

CLINICAL TRIAL NUMBER:

Not applicable

CONSENT TO PUBLISH DECLARATION:

The authors declare that this article has not been submitted to or published in another publisher.

ETHICS AND CONSENT TO PARTICIPATE DECLARATIONS:

Not applicable

References

[1] Walls, D., Smith, J., & Liu, Y. (2024). Advances in multistage centrifugal pump design for variable load applications. *Preprints*, 202404.1817.

[2] Zhou, J., Zhang, L., & Wang, S. (2019). Integrated optimization of surface pipeline network and subsurface reservoir for water flooding. *Energy, 176*, 545–559.

[3] Elembaby, M., El-Banbi, A., & El-Sayed, A. (2023). Optimization of surface facility design for mature waterfloods using lifecycle cost analysis. *SPE Production & Operations, 38*(02), 150–162.

[4] De Oliveira, L. P., Silva, R., & Santos, M. (2025). Thermodynamic analysis of throttling losses in high-pressure hydraulic systems. *Applied Thermal Engineering, 215*, 118–129.

[5] Rossini, M., D'Orazio, A., & Bortolin, S. (2020). Impact of injectivity decline on centrifugal pump reliability in water injection systems. *Wear, 442*, 203–214.

[6] Obibuike, U. J., Igbojionu, A. C., & Kerunwa, A. (2022). Simulation studies on comparative evaluation of water injection and gas injection for pressure maintenance. *Petroleum Science and Technology, 40*(3), 285–302.

[7] Aladeitan, Y. M., Uwaforo, O., & Adewale, K. (2020). Integrated reservoir management in a Niger Delta oil field: A case study of rising water cut challenges. *Journal of Petroleum Exploration and Production Technology, 10*(5), 2101–2115.

[8] Wan, J., Li, X., & Dai, H. (2023). Digital twin framework for predictive maintenance of offshore oil and gas production equipment. *Ocean Engineering, 268*, 113393.

[9] Gao, J., Wang, H., & Liu, Y. (2023). Carbon footprint modeling and reduction strategies for water flooding oilfields. *Energy Reports, 9*, 345–356.

[10] Gómez-Gardars, E., Rodríguez-Macias, A., et al. (2022). Assessment of the water–energy–carbon nexus in energy systems: A multi-objective approach. *Applied Energy, 305*, 117872.

[11] Li, W., Zhang, Q., & Zhou, B. (2024). Vibration signature analysis of multistage centrifugal pumps under variable flow conditions. *Mechanical Systems and Signal Processing, 185*, 109812.

[12] Simon, X., Meck, K., & Brecht, B. (2021). Failure mechanisms of mechanical seals in variable speed pump applications. *Tribology International, 153*, 106603.

[13] Wang, S., Liu, Z., & Zhao, H. (2025). Thermally induced fracture modeling during long-term water injection using a thermo-hydro-mechanical phase-field model. *International Journal of Rock Mechanics and Mining Sciences, 186*, 105–118.

[14] Nwokoma, P. O., & Dagde, K. K. (2024). Characterization of produced water properties and valve trim erosion in Niger Delta flow stations. *American Journal of Chemical Engineering, 12*(4), 12–25.

[15] National Electrical Manufacturers Association (NEMA). (2024). *ANSI/NEMA MG 1-2024: Motors and Generators*. Rosslyn, VA.

[16] Aledan, I. D. (2023). Techno-economic assessment of produced water management strategies in mature fields. Doctoral dissertation, University of Lagos.

[17] Horn, S., Ivantysyn, R., & Weber, J. (2022). Tribo-optimized lubricating interfaces in hydrostatic pumps with surface shaped slippers. *13th International Fluid Power Conference (IFK)*, Aachen, Germany.

[18] Luo, Y., Zhang, W., Fan, Y., Han, Y., Li, W., & Acheaw, E. (2021). Analysis of Vibration Characteristics of Centrifugal Pump Mechanical Seal under Wear and Damage Degree. *Shock and Vibration, 2021*, 6670741.

[19] Wang, G., Ghoddousi, S., Wang, Z., & Song, L. (2022). Development, Validation and Application of an Energy Model for Energy Efficient Operation of Parallel Pump Systems. *Journal of Building Engineering*, Elsevier Pre-print.

[20] Zhao, C., Wang, J., Fan, X., Tian, G., & Zheng, H. (2025). Experimental Analysis and Temperature Rise Modeling of Multistage Centrifugal Pumps for Solar Ejector Refrigeration Systems. *Energies, 18*, 6367.

[21] Zou, J., Luo, Y., Han, Y., Fan, Y., & Wang, C. (2025). Investigation on the Vibration Induced by the Rotary-Shaft-Seal Condition in a Centrifugal Pump. *Sensors, 25*(17), 5399.

[22] Wang, Y., Zhang, H., Han, Z., & Ni, X. (2021). Optimization Design of Centrifugal Pump Flow Control System Based on Adaptive Control. *Processes, 9*(9), 1538.

[23] Jia, D., Liu, H., Zhang, J., Gong, B., Pei, X., Wang, Q., & Yang, Q. (2020). Data-driven optimization for fine water injection in a mature oil field. *Petroleum Exploration and Development, 47*(3), 674-682.

[24] Wang, J., Li, X., & Zhang, Y. (2024). The injection capacity evaluation of high-pressure water injection in low permeability reservoirs: Numerical and case study. *Frontiers in Earth Science, 12*, 1411451.

[25] American Petroleum Institute. (2021). *API Standard 610: Centrifugal Pumps for Petroleum, Petrochemical and Natural Gas Industries* (12th ed.). Washington, DC: API Publishing Services.

[26] Chen, Q., Li Huan, Y., Zhi Peng, Q., Cong Xin, Y., & Chen Hui, N. (2022). Flow mechanism and axial force distribution characteristics of multistage pump cavity. *Science Progress, 105*(4).

[27] Al-Fatlawi, O. (2022). Artificial intelligence-based smart water injection system for reservoir pressure maintenance. *Journal of Petroleum Science and Engineering, 208*, 109638.